ELSEVIER

Journal of Chromatography A, 807 (1998) 185–207

JOURNAL OF CHROMATOGRAPHY A

Comparison of diffusion and diffusion–convection matrices for use in ion-exchange separations of proteins

Dominic C. Nash*, Howard A. Chase

Department of Chemical Engineering, University of Cambridge, Pembroke Street, Cambridge CB2 3RA, UK

Received 14 November 1997; received in revised form 13 January 1998; accepted 26 January 1998

Abstract

A comprehensive study has been undertaken to characterise a range of chromatographic properties for a series of modified polystyrene–divinylbenzene (PS–DVB) chromatography matrices. The matrices studied included diffusion matrices and matrices that allowed convective mass transfer of liquid into the particles at high flow-rates, so-called ''perfusion'' matrices. The matrices tested included the following: CG1000sd 20–50 μm (TosoHaas), PLRP4000s 15–25 μm, 50–70 μm (Polymer Labs.), Source 15RPC and 30RPC, 15S, 30S, (Pharmacia Biotech), POROS 20SP type 1 matrix and OH activated POROS 20 type 2 matrix (PerSeptive Biosystems) and SP Sepharose Fast Flow (Pharmacia Biotech). A Van Deemter equation was used to determine bead tortuosities and split ratios. Frontal analysis, resolution studies, ionic capacities and isotherms were measured. It was found that diffusion–convection chromatographic particles had smaller plate heights to comparable diffusion particles. The smallest diffusion bead, Source 15, had the lowest plate heights at low superficial velocities, but the small particle size resulted in a high back pressure at high flow-rates. The equilibrium binding capacities for lysozyme and IgG on the diffusion–convection matrices were substantially lower than the equilibrium binding capacities on the diffusion matrices. The dynamic capacities for these proteins were also lower on the diffusion–convection particles, compared to the diffusion particles, over the tested flow-rates. At high protein loading, resolution between proteins was higher on diffusion particles than on diffusion–convection particles. Diffusion–convection particles showed low or no resolution at high protein loading. At analytical level loadings, the diffusion–convection particles achieved a high resolution over the whole flow-rate range tested and were more suitable for this application than diffusion particles.

Keywords: Diffusion matrices; Diffusion–convection matrices; Stationary phases, LC; Proteins

1. Introduction

The development of rigid chromatographic supports, such as silica or polymer based matrices such as polystyrene, has dramatically reduced the processing time required to separate proteins. The high compressibility of softer matrices such as agarose, even when highly crosslinked, limits their uses in rapid separations.

Polystyrenic matrices were first developed in 1964 by Moore [1] and these crosslinked porous particles are rigid and non-compressible, even at high flow-rates. These polystyrenic matrices need modification to eliminate non-specific protein binding, and various methods of rendering the particle surface hydrophilic, and therefore suitable for use in protein separations, have been employed [6,9,21]. Recently,

*Corresponding author.

0021-9673/98/$19.00
PII: S0021-9673(98)00076-4

there have been attempts to increase the rate at which protein separation on modified polystyrenic matrices can be achieved. The main approaches have been to either create non-porous micro-particles, which have a diameter small enough to ensure a sufficient external surface area [2,3], or to encourage convective mass transfer into the bead interior by creating matrices that contain large through pores (>5000 Å) connected to smaller diffusional pores (300–700 Å) to provide an adequate surface area. These diffusion–convection particles are sometimes called ''perfusion'' matrices and were developed in the early 1990s [4–6]. At high flow-rates, these diffusion–convection particles allow convective mass transfer into the particle interior and diffusional mass transfer becomes less significant. It is thought that the amount of solute transported into the particle interior by convective means is proportional to flow-rate and at high flow-rates the column plate height due to throughpore mass transfer resistances will become effectively independent of flow-rate [7]. Diffusion–convection particles are hindered by a lack of surface area resulting from the need for the presence of larger pores and conventional, diffusion matrices can be expected to have a higher total protein binding capacity. This has prompted a different type of diffusion–convection matrix to be developed by PerSeptive Biosystems, POROS type 2 media [8] which have smaller through pores than the original POROS type 1 diffusion–convection matrices. POROS type 1 matrices have a lower adsorption capacity but faster adsorption kinetics whilst POROS type 2 matrices have a higher binding capacity but slower adsorption kinetics.

In analytical chromatography, the most desirable characteristic is the rapid transfer of protein from the bulk liquid phase to the binding sites in the beads in order that the separation can be conducted in the minimum time. The presence of a large total surface area is not the main factor in determining the matrix suitability. In preparative chromatography, however, the matrix requirements are for rapid transfer of protein to the bead binding sites and a high available particle surface area to enable a high total binding capacity per unit volume of adsorbent bed. By using diffusion–convection particles or non-porous particles (which eliminate the limitations of intra-particle mass transfer), there will be a compromise between the rate at which protein can be adsorbed and the total amount of protein that can be adsorbed.

The central purpose of this paper is to investigate the differences between diffusion–convection polystyrenic matrices and diffusion polystyrenic matrices in order to determine the degree of suitability of these matrix types in different chromatographic regimes. Analytical and preparative chromatography techniques have been compared for a range of sulphopropyl (SP) or sulphonate (S) derivatised cation ion-exchange media, both commercially acquired, and media created from crosslinked polyvinyl alcohol (PVA) coated polystyrene–divinyl benzene (PS–DVB) base matrices, as previously described [9,10]. SP ion-exchange functionalities were derivatised onto the PVA modified matrices as described by McCreath et al. [11]. These SP and S derivatised PS–DVB based matrices were also compared to SP Sepharose Fast Flow, a popular low/medium pressure matrix used in the preparative purification of proteins.

Each matrix was examined to determine its pressure drops and compressibility when used in packed beds. The variation of plate heights with flow-rate were established for two proteins (lysozyme and IgG) on each bed and the suitability of an extended Van Deemter model as summarised by Rodrigues [12] and derived by Carta and Rodrigues [28] was determined. The split ratio, apparent matrix tortuosity and protein diffusivity into the matrices were determined. Ionic capacities, isotherm characteristics for lysozyme and IgG and the dynamic capacities of these matrices for these proteins at various flow-rates were measured. Finally the resolution of the two proteins, lysozyme and cytochrome *c* were measured for beds of each adsorbent to examine the effects of increasing protein load and flow-rate.

2. Experimental

2.1. Materials

CG1000sd matrices were purchased from TosoHaas (Philadelphia, PA, USA). PLRP4000s, 15–25 μm and 50–70 μm were kindly donated by Polymer Labs. (Church Stretton, Shropshire, UK). POROS 20SP type 1 and OH-activated POROS 20

type 2 matrices were purchased from PerSeptive Biosystems (Cambridge, MA, USA). Source 15RPC, Source 30RPC, Source 15S and Source 30S were kindly donated by Pharmacia Biotech (Uppsala, Sweden) and SP Sepharose Fast Flow was obtained from Pharmacia Biotech (St. Albans, UK).

Chicken egg white lysozyme (M_r 14 300, p*I* 11.0), horse heart cytochrome *c* (M_r 13 000, p*I* 10.6) were obtained from Sigma (Poole, Dorset, UK). Human immunoglobulin G (IgG) (M_r 150 000, p*I* 6.4–7.2) was obtained from Pharmacia Biotech (Uppsala, Sweden).

PVA (M_r 13 000–23 000, 87–89% hydrolysed) was purchased from Aldrich (Gillingham, Kent, UK) as were HCl (5 *M*), sodium hydroxide, iodine, potassium iodide, methanol, disodium hydrogenorthophosphate, sodium hydrogenphosphate, 3-amino-1-propanesulphonic acid, cyanuric chloride and acetone. Boric acid (99.5% purity) and glutaraldehyde were purchased from Sigma.

2.2. Instrumentation and columns

Chromatography was carried out on a Pharmacia FPLC system (fast protein liquid chromatography) categorised as 2xP-6000 pumps, UV-1, Frac-100, Rec-482 obtained from Pharmacia LKB (Uppsala, Sweden). Two different columns were used, namely a HR5/5 column (50×5 mm, 1 ml column volume) and a HR5/10 column (100×5 mm, 2 ml column volume). UV–Vis spectrophotometry was carried out using a Shimadzu UV-160A (VA Howe, UK). Scanning electron microscopy (SEM) was carried out on a JSM-820 scanning microscope (JEOL, Japan). Particle size analysis was performed on a Helium Neon Laser-Optical Diffraction Spectrometer (Sympatec, Germany).

2.3. Methods

2.3.1. SP-PVA modification of PS–DVB base matrices

The commercially-available SP or S derivatised modified polystyrenic matrices did not need any further modification. These matrices included Source 15S, Source 30S [the sulphonate groups on both of these matrices being connected to the matrix with a hydrophilic spacer arm ($-CH_2-O-CH_2-CHOH-CH_2-O-CH_2-CHOH-CH_2-SO_3^-$)]. POROS 20SP matrices had been derivatised with sulphopropyl groups ($-CH_2-CH_2-CH_2-SO_3^-$). Native polystyrenic matrices required PVA modification to render them hydrophilic and these modified matrices included Source 15RPC, Source 30RPC, CG1000sd, PLRP4000s 15–25 μm and PLRP4000s 50–70 μm matrices. Once these matrices had been modified they were derivatised with SP ion-exchange groups and the nomenclature used to describe them is SP-PVA-bead type. POROS 20 OH activated matrices were supplied already modified with a hydrophilic surface, but no functional groups had been derivatised onto these particles. On this matrix, only SP derivatisation was carried out.

The PVA coating procedure was essentially the same as described in previous papers [9,10]. The optimum shielding of the PS–DVB surface using a PVA coating technique was obtained by adsorbing PVA (M_r 13 000–23 000, 87–89% hydrolysed) and then subsequent crosslinking with glutaraldehyde at a crosslinking ratio of 50 mol glutaraldehyde/mol PVA.

SP derivatisation is described in a previous publication [11]. PVA–PS–DVB particles (5 ml settled volume) were washed with ice cold NaOH (0.75 *M*, 500 ml) over a number 2 sintered disk for 30 min. Ice cold cyanuric chloride (50 m*M*) in acetone (250 ml) was slowly poured over the wet particles for 20–25 min. After activation with cyanuric chloride the PVA–PS–DVB matrices were then washed with 10 ml of ice cold distilled water and then immediately added to 3-amino-1-propanesulphonic acid (0.5 g) in Na_2HPO_4 (1 *M*, 10 ml, final pH 9.1). The suspension was stirred overnight at 40°C and then for 5 h at 60°C. After immobilisation, the SP-PVA–PS–DVB matrices were washed on a sinter (grade 2) with distilled water (200 ml), NaOH (0.4 *M*, 200 ml) and finally with distilled water (200 ml).

The POROS 20 OH activated type 2 media was derivatised with SP groups in the same way as the PVA-modified PS–DVB matrices.

2.3.2. Scanning electron microscopy

The SP derivatised modified polystyrenic matrices were dried at 60°C for 1 week. The samples were then prepared for SEM by coating with gold and then loaded into a JSM-820 scanning microscope (JEOL,

Japan) and images were photographed using a voltage of 10 kV.

2.3.3. Pressure drops and compression

The derivatised chromatography matrices were loaded into an HR5/10 column (100×5 mm, 2 ml volume) and 20 m*M* phosphate buffer, pH 6.0 was pumped through the column at varying flow-rates (0.5, 1, 2, 4 and 8 ml/min corresponding to superficial velocities of 153, 306, 611, 1222 and 2445 cm/h). Short segments of large diameter tubing (1.9 mm) were used to minimise extra-column effects. The back-pressure on the pumps were noted and the height of the column was measured. Permeability was calculated using Darcy's Law which relates pressure drop across a packed bed to superficial velocity with the equation:

$$u = K\frac{-\Delta P}{L_0} \tag{1}$$

where u is the superficial velocity through the bed, K is the bed permeability, $-\Delta P$ is the pressure drop across the column and L_0 is the bed length. The permeability parameter is a useful measure of the resistance of the column to flow, and permeability is a function of bed voidage, particle diameter and liquid viscosity.

2.3.4. Plate height measurements

Plate heights are a function of column efficiency and describe the degree of band broadening of a solute as it passes through a column and associated tubing. To determine the overall column efficiency a solute of small molecular mass is used, as this will have a high diffusivity and can penetrate most of the matrix. However, macromolecules have a lower diffusivity and will usually be associated with higher plate heights. All experiments were conducted under conditions where protein solutes would not be retained by the ion-exchange groups [(1.5 *M* NaCl in 20 m*M* phosphate buffer pH 6.0) on HR5/10 columns (100×5 mm, 2 ml volume)]. The overall column efficiency and peak symmetry were determined by pumping a pulse of $NaNO_3$ (10 mg/ml, 25 μl) at 0.5 ml/min (153 cm/h) through the column. Short segments of small diameter tubing (0.5 mm) were used to minimise extra-column effects. Column efficiency with protein solute was determined by pumping a pulse of protein [lysozyme or IgG (1 mg/ml, 25 μl)] through the column at varying flow-rates (0.5, 1, 2, 4 and 8 ml/min corresponding to superficial velocities of 153, 306, 1222 and 2445 cm/h).

Each solute peak was analysed to assess the asymmetry factor. This determined the suitability of the bed to be described as a series of plates, as non-Gaussian peaks should not be used in plate theory analysis [24]. The asymmetry factor was calculated from the following equation and peaks with asymmetry factors outside of the range 0.8–1.3 were not used in subsequent analysis.

$$S = \frac{b_{0.1}}{a_{0.1}} \tag{2}$$

S is the peak symmetry coefficient, $a_{0.1}$ is the distance between the peak front and peak maximum at 0.1 peak height and $b_{0.1}$ is the distance between the peak maximum and peak tail at 0.1 peak height.

For Gaussian shaped peaks the number of theoretical stages present in the column can be calculated from the residence time and the peak width variance as indicated in Eq. (3).

$$N = \left(\frac{t_r^2}{\sigma^2}\right) = 5.54\left(\frac{t_r}{w_{0.5}}\right)^2 \tag{3}$$

where N is the number of theoretical plates, t_r is the mean residence time (t_r is the first absolute moment) and σ^2 is the peak width variance (σ^2 is the second central moment). Where t_r is the retention time and $w_{0.5}$ is the width of the peak at half peak height. The plate height can then be determined from the following equation:

$$H = \frac{L_0}{N} \tag{4}$$

where H is the plate height (mm) and L_0 is the length of the column (100 mm) and N is the number of plates in the column.

2.3.4.1. Van Deemter analysis

The variation of plate height obtained for lysozyme and IgG on each bed at differing flow-rates was modelled using a modified Van Deemter equation based on previous work [8,28]. The basic Van

Deemter equation describes the band broadening processes involved in diffusion chromatography and can be represented by the following equation:

$$H = A + \frac{B}{u} + (C_f + C_p + C_{ads})u \quad (5)$$

where H is the column plate height, u is the superficial velocity, A corresponds to inequalities in patterns of flow in column packing (i.e., a packing constant), the B/u term corresponds to the axial diffusion in mobile phase, the C_f term corresponds to the plate height associated with the mass transfer of solute in the external stationary phase film, the C_p term is the plate height associated with the mass transfer of solute to and from the binding sites in the stationary phase including diffusion through the stagnant mobile phase in the intra-particle pores and the C_{ads} term is the plate height associated with the kinetics of solute adsorption onto the stationary surface.

This Van Deemter equation can be simplified. In liquid chromatography (LC) the B parameter is usually small and even at moderate flow-rates the corresponding term tends towards zero. The external film mass transfer resistance is small and can be neglected because its contribution to the overall mass transfer resistance of highly porous particles has been found, for most systems of practical importance, to be negligible [25,26]. With fast adsorption–desorption kinetics, the plate height associated with solute adsorption resistance reduces to zero. The simplified Van Deemter equation thus becomes:

$$H = A + C_p u \quad (6)$$

Expanding Eq. (6) as formulated by Schneider and Smith [27], yields an expression describing plate heights for conventional, diffusion chromatographic supports:

$$H = A + \frac{2}{15}\frac{(1-\varepsilon)\varepsilon_p R_p^2 (1+K)^2}{D_p(\varepsilon + (1-\varepsilon)\varepsilon_p(1+K))^2}u \quad (7)$$

where u is the superficial velocity of the mobile phase D_p is the pore diffusivity, R_p is the particle radius, ε is the interstitial void fraction in the bed, ε_p is the particle porosity and K is the Henry's Law constant ($K=0$ for unretained adsorbate).

Van Deemter equations had to be modified to describe column plate height with diffusion–convection supports. Plate heights on monodisperse pore diffusion–convection supports can be described using the following equation, neglecting axial molecular diffusion resistance, adsorption kinetic resistances and external film mass transfer resistance terms [8,12,29]:

$$H = A + \frac{2(1-\varepsilon)\varepsilon_p (1+K)^2 R_p^2 f(\lambda)}{15 D_p(\varepsilon + (1-\varepsilon)\varepsilon_p(1+K))^2}u \quad (8)$$

Diffusion–convection supports, however, are thought more accurately to possess a bidisperse pore structure in which more than one resistance to mass transfer occurs. Afeyan et al. [4] have described these supports as containing a network of throughpores transecting a network of smaller pores. Carta and Rodrigues [28] developed a plate height model which describes mass transfer of solute into diffusion–convection supports with a bidisperse pore structure:

$$H = A + \frac{2(1-\varepsilon)\varepsilon'(b)^2 R_p^2}{15 D_p(\varepsilon + (1-\varepsilon)\varepsilon'(b))^2}\left[f(\lambda) + \frac{b-1}{b^2 T} \right]u \quad (9)$$

where ε' is the throughpore voidage and $f(\lambda)$ is the convective enhancement factor:

$$f(\lambda) = \left(\frac{3}{\lambda}\left[\frac{1}{\tanh(\lambda)} - \frac{1}{\lambda}\right]\right) \quad (10)$$

λ is the intra-particle Peclet number

$$\lambda = \frac{v_p a}{D_p} \quad (11)$$

where a is the characteristic dimension of the particle ($a = R_p/3$) [12], v_p is the intra-particle velocity, derived from the split ratio value, α, i.e., the volume fraction of mobile phase that flows through the media.

$$v_p = \frac{\alpha}{(1-\varepsilon)\varepsilon'}u \quad (12)$$

b is defined as:

$$b = 1 + \frac{(1-\varepsilon')K'}{\varepsilon'} \quad (13)$$

where K' is the distribution coefficient between the throughpore fluid and the microparticle, i.e., $q =$

$K'c'$, where q is the total solute concentration in the microparticle and c' is the concentration of solute in the throughpores. The total solute concentration in the microparticle includes the solute in the microparticle pores as well as solute adsorbed on the microparticle surface. For unretained solutes, $K' = \varepsilon''$, where ε'' is the microparticle porosity.

In Eq. (9), T is the ratio of diffusional time constants for the overall particle and microparticle and is defined as:

$$T = \frac{(D_c/R_m^2)}{(D_p/R_p^2)} \tag{14}$$

where D_c is the microparticle diffusivity based on the total solute concentration in the microparticle (as defined by Carta and Rodrigues [28]), R_m is the microparticle radius, D_p is the particle pore diffusivity and R_p is the particle radius.

The effect of convective flow into monodisperse pore, diffusion–convection support particles is such that at high superficial velocities, Eq. (8) reaches an asymptote whereby plate height becomes independent of flow-rate [8,12]. In media where there is little convective flow through the particles (i.e., diffusion particles or diffusion–convection particles operating at low superficial velocities), the enhancement factor, $f(\lambda)$, tends towards 1 and the Van Deemter equation becomes identical to that expected for purely diffusion media, Eq. (7). However, in a bidisperse pore diffusion–convection support, the contribution to the overall plate height arising from microparticle pore diffusion depends on the superficial flow velocity and plate height cannot be truly independent of flow-rate. The effect of microparticle pore diffusivity on the dynamic performance of columns containing diffusion–convection particles, however, is often small [25] and its contribution to the overall plate height only becomes significant at very high flow-rates [28]. It can be seen, for example, that with a particle with characteristics $R_p = 10$ μm, $R_m = 0.5$ μm, $\alpha = 0.004$, $\varepsilon = 0.35$, $\varepsilon' = 0.4$, $\varepsilon'' = 0.4$, $D_p = 4 \cdot 10^{-11}$ m^2/s, $D_c/D_p = 0.2$ and under unretained conditions ($K' = \varepsilon'$) then for the plate height associated with microparticle diffusion to be 10% that of the plate height associated with particle throughpore diffusion and convection, a mobile phase superficial velocity of 28 000 cm/h is required.

If in Eq. (9) the contribution to plate height from microparticle diffusion can be neglected then the plate height of a bidisperse pore structure support with diffusion–convection characteristics is approximately (neglecting axial molecular diffusion resistance, adsorption kinetic resistances and external film mass transfer resistance terms [8,12,29]):

$$H = A + \frac{2(1-\varepsilon)\varepsilon' b^2 R_p^2 f(\lambda)}{15 D_p (\varepsilon + (1-\varepsilon)\varepsilon'(b))^2} u \tag{15}$$

where the convective enhancement factor, $f(\lambda)$, is calculated as described in Eqs. (10)–(12). At high mobile phase velocities (but at flow-rates below which microparticle pore diffusion effects become significant) Eq. (15) predicts a plate height which is effectively independent of flow-rate. At low flow-rates Eq. (15) tends towards the form of the Van Deemter equation expected for diffusion media. If the microparticle voidage approaches zero, Eq. (15) is the same as Eq. (8) which describes the variation of plate height with flow-rate for monodisperse particles.

The pore diffusivity, D_p, is the diffusion coefficient of the protein within the pores of the particle, and is different from the effective bead diffusivity. The pore tortuosity factor is a ratio of the rates of transfer of protein through the free liquid compared to transfer of protein through the pores and is described by:

$$\tau' = \tau^2 = \frac{D_{free}}{D_p} \tag{16}$$

where τ' is the tortuosity factor, τ is the pore tortuosity, D_{free} is the free diffusion coefficient and D_p is the pore diffusion coefficient.

2.3.4.2. Calculation of support characteristics

Supports displaying a monodisperse pore structure were analysed using the monodisperse plate height equation, Eq. (8), which, as intra-particle convection tends towards zero, is equivalent to an equation describing plate heights with a purely diffusive support. Supports displaying a bidisperse pore structure were analysed using the bidisperse plate height equation, Eq. (9).

The interstitial bed voidage, ε, was estimated to be 0.35 [31], for all adsorbents with the exception of the

beds of monosize Source beads whose interstitial voidage was estimated to be 0.4 [30]. The total pore voidage of all the particles, ε_p, was measured experimentally for each support type and it was found that all the PS–DVB based supports had a porosity between 0.6–0.65 and the porosity of the SP Sepharose Fast Flow supports was found to be 0.88. The throughpore voidage, ε', of the diffusion–convection particles has been estimated to be 0.6 [8], 0.5 [4], 0.45 [32], 0.4 [28] and 0.35 [15]. It was decided in these studies to assume that the throughpore and microparticle voidage were the same value and so it was decided to have a throughpore and microparticle voidage of 0.4. This value means that the total particle porosity of the PS–DVB based supports with a bidisperse pore structure was 0.64. The PS–DVB supports with diffusion characteristics were analysed using a porosity of 0.6.

The split ratio, packing constant and effective pore diffusivity were calculated using parameter regression between experimental values and calculated Van Deemter values as outlined by McCoy et al. [8]. The particle split ratio, packing constant A and pore diffusivity were initially estimated, and through an iterative procedure were altered to minimise the square of the difference between the calculated values and the experimental values.

2.3.5. Ionic capacities

The number of SP or S groups derivatised onto the particles were determined by a titration method initially outlined by Helfferich [13]. The procedure involved washing the cation exchangers in an HR5/10 column with 2 *M* HCl (50 ml) and then with ultrapure water (100 ml). The washed support was then transferred to 10 ml of 0.1 *M* NaOH containing 0.5 *M* NaCl in a test tube. The sealed test tube was mixed gently overnight on a rotating mixer, centrifuged and then 5 ml of supernatant was removed into a 50-ml conical flask containing one drop of phenolphthalein solution. The mixture was then back titrated with 25 m*M* HCl solution from a 25-ml glass burette and the volume of acid used was noted.

2.3.6. Isotherm calculations

Aliquots (0.1–0.2 ml) of settled ion-exchange matrices were equilibrated with 20 m*M* phosphate buffer pH 6.0 and added to a series of test tubes. Protein solution (2 ml, 0.2–12 mg/ml) of either lysozyme or IgG was added to each tube. The tubes were sealed and rotated overnight after which the supernatant was assayed at 280 nm for protein concentration. The A_{280} value was used to calculate protein concentration by employing extinction coefficients of 2.64 and 1.23 ml/mg/cm for lysozyme and IgG, respectively [14]. The Langmuir isotherm has been used to describe protein adsorption to a variety of adsorbents, including ion-exchangers and affinity adsorbents [22,23]. The amount of protein that adsorbed to the matrix was calculated from a mass balance and the data obtained was fitted to a linearised version of the Langmuir Equation.

The Langmuir equation can best be described for protein adsorption as:

$$C_s = \frac{Q_m C}{K_d + C} \tag{17}$$

where C_s is the concentration of bound protein, C is the concentration of free protein in solution, Q_m is the maximum binding capacity and K_d is the dissociation constant.

2.3.7. Protein recoveries

Each ion-exchange matrix was loaded into an HR5/5 (50×5 mm, 1 ml column volume) column and 1 ml of protein solution (8 mg/ml) of either lysozyme or IgG was applied to the column in 20 m*M* phosphate buffer pH 6.0. The protein was then eluted by applying 1.5 *M* NaCl in 20 m*M* phosphate buffer, pH 6.0, to the column until the absorbance of the outlet stream approached zero. The two fractions: adsorption and elution, were collected and assayed at 280 nm to determine the protein concentration. The amount of protein that eluted from the column was compared to the amount that was estimated to have been adsorbed. The procedure was repeated four times for each protein.

2.3.8. Frontal analysis

Either lysozyme or IgG solution in 20 m*M* phosphate buffer pH 6.0 was placed into a 50-ml Superloop for subsequent loading onto the respective SP or S derivatised bed. The concentration of the applied protein solution was 1 mg/ml for most matrices. However, the capacity of the Superloop at a protein

concentration of 1 mg/ml is 50 mg and the commercially acquired S and SP matrices had dynamic capacities greater than 50 mg. For these matrices a protein concentration of 2 mg/ml was used. The protein solutions were applied to SP and S derivatised matrices in a HR5/5 column (50×5 mm) at flow-rates in a strict order of 1, 1, 0.5, 2, 4, 8 and 1 ml/min corresponding to a superficial velocity of 306, 306, 153, 611, 1222, 2445 and 306 cm/h. The dynamic capacities of the SP and S derivatised matrices for the first two runs and the final run [all conducted at 1 ml/min (306 cm/h)] were compared to ensure that the dynamic capacities were reproducible even after the bed had been operated under a high flow-rate.

Dynamic capacities were calculated by determining the volume of protein solution applied to the bed at the point where the outlet concentration was 5% that of the feed stream and deducting from this the volume of protein solution still in the system voids. The void volume determined from frontal analysis of the system with protein under non-adsorbing conditions was estimated to be 0.81 ml for lysozyme and 0.65 ml for IgG.

The protein solution was applied to the column until the absorbance of the outlet stream approached that of the feed stream. At this point the column was washed with 20 ml of adsorbent buffer (2 ml/min, 611 cm/h) and then the adsorbed protein was eluted with 1.5 *M* NaCl in 20 m*M* phosphate buffer pH 6.0 (2 ml/min, 611 cm/h). The liquid from these three stages was collected in three distinct fractions: the adsorption, wash and elution stages. Protein concentration in each of these three fractions was determined by measuring the absorbance at 280 nm. The saturation capacities and recoveries were estimated from the protein concentrations of these three fractions and compared to the protein adsorption isotherm value and expected recovery of the bed.

2.3.9. Resolution of protein peaks

Each SP or S derivatised matrix was loaded into an HR5/10 column (100×5 mm, 2 ml bed volume) and a volume of cytochrome *c* and lysozyme solution in 20 m*M* phosphate buffer pH 6.0 was applied to the column (total protein mass loading 0.05 mg, 0.5 mg, 2.5 mg, 5.0 mg, 10.0 mg and 20.0 mg, lysozyme and cytochrome *c* at equal concentrations). The protein mixture was applied at a flow-rate of 1 ml/min, i.e., 306 cm/h. After the proteins had been applied, the column was washed with 4 ml of buffer (1 ml/min, 306 cm/h) and then a buffer gradient was applied to the column, with a gradient change of 0–1 *M* NaCl in 20 m*M* phosphate buffer pH 6.0 in 12 column volumes (24 ml). For the SP-PVA Source matrices only, the gradient was 0–1.5 *M* NaCl in 20 m*M* phosphate buffer pH 6.0 in 12 column volumes (24 ml) as lysozyme had only partially eluted at a salt concentration of 1 *M*. The buffer gradient was applied at flow-rates of 1, 2, 4 and 8 ml/min, corresponding to superficial velocities of 306, 611, 1222 and 2445 cm/h.

The optical absorbance of the outlet stream at 280 nm was measured by flow spectrophotometry and the resolution was calculated from the resultant concentration profile using the equation:

$$R = 2\frac{t_{r2} - t_{r1}}{w_1 + w_2} \tag{18}$$

where R is the resolution, t_{r1} and t_{r2} are the retention times of peak 1 and 2, respectively and w_1 and w_2 are the widths of peaks 1 and 2 at the absorbance baseline. For peaks that went above the maximum absorbance limit of the UV detector, retention times were estimated to be at the mid-point of the peaks.

3. Results

3.1. Characterisation of SP or S derivatised particles

Fig. 1 shows SEM photographs of the chromatography matrices used in this study. Only one set of Source 15 and Source 30 beads are shown in Fig. 1 as the SP-PVA-Source matrices looked identical to the equivalent commercial Source S matrices. It can be seen that the diffusion beads have substantially different pore sizes to the diffusion–convection matrices. The pore size of the Source 15 particles appear larger than the pores of the Source 30 beads and the Source 15 pores are comparable with those found in the CG1000sd matrices. The through pores for the PLRP matrix look larger than the POROS type 1 matrix, and the latter matrix has larger pores

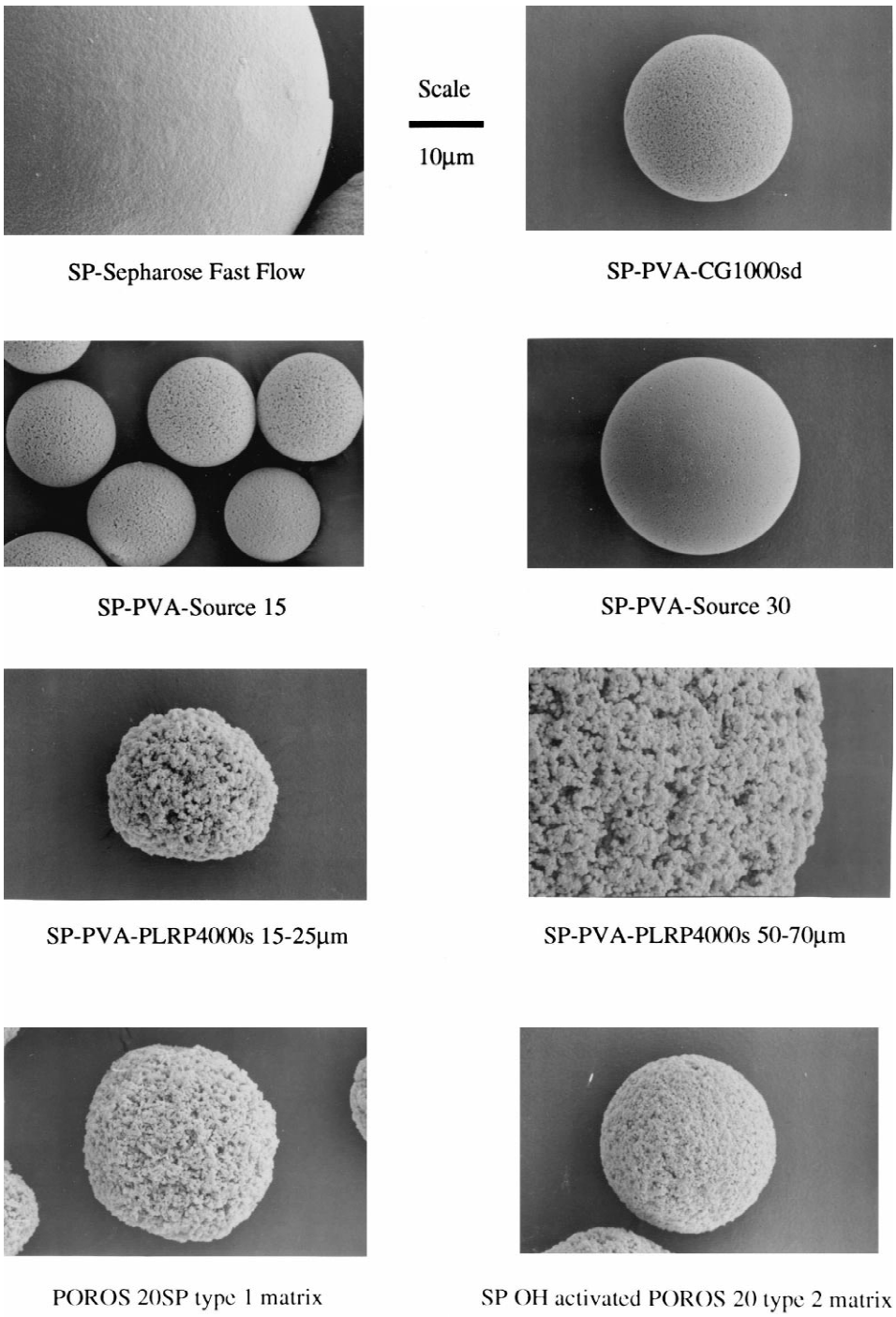

Fig. 1. SEMs of the chromatographic supports. The initial image was photographed at a magnification of ×2500. All bead types were photographed at the same magnification and are therefore directly comparable.

than the POROS type 2 matrix. SP Sepharose Fast Flow was also characterised using SEM and it was noticed that substantial shrinkage occurred in preparing the sample. The fully hydrated SP Sepharose Fast Flow particles are likely to show a larger pore size than was seen in Fig. 1.

3.2. Particle sizes, pressure drops and compressions

Table 1 shows for each adsorbent the particle size, bed permeability and bed compression values. The permeabilities were found to alter between the beads, as expected due to the large particle size differences. However there seemed to be an unanticipated discrepancy between the SP beads derivatised by us using a PVA modification technique and those which are commercially available. The SP-PVA matrices had higher permeabilities than the equivalent commercial SP or S matrices and this could be due to the commercial beads packing within a bed to a lower voidage than the beads modified using PVA. The Source 15S matrices could not have buffer applied at a flow-rate of 2445 cm/h as the back pressure was greater than 30 bar (FPLC pressure operation is less than 30 bar). Increase of the rates of mass transfer into chromatographic particles by reducing particle size has drawbacks if the operating system is not able to cope with the increased pressure drop.

All the modified PS–DVB matrices show low degrees of compression, especially when compared to SP Sepharose Fast Flow. With a pressure drop of just 0.6 bar/cm there is a 5% reduction in column volume of SP Sepharose Fast Flow compared to negligible compression for the PS–DVB matrices (the maximum operating pressure of SP Sepharose Fast Flow is recommended to be no more than 0.3 bar/cm [16]). At a pressure drop of 1 bar/cm, the PS–DVB showed a compression of about 1.0% and at pressure drops approaching 3 bar/cm the compression was still only about 3%. PS–DVB beads can therefore be operated under high pressure drops with little compression.

Table 1
Physical characteristics of chromatography matrices

Bead name	Type of chromatography bead	Average particle diameter (volume median) (μm)	Bulk density (g dry bead/ml settled bed) (g/ml)	Bed permeability ($cm^2/h/bar$)	Pressure drop across 10 cm bed at 306 cm/h (bar)	Compression (%)	Pressure drop across 10 cm bed at 1222 cm/h (bar)	Compression (%)	Pressure drop across 10 cm bed at 2445 cm/h (bar)	Compression (%)
SP Sepharose Fast Flow	Diffusion	98.8	0.132	66.2[a]	0.8	0.0	2.0	2.0	6.0	5.0
SP-PVA-CG1000sd	Diffusion	34.5	0.329	18.4	1.7	0.0	6.2	0.5	13.8	1.0
SP-PVA-Source 15	Diffusion	15.5	0.340	9.5	3.0	0.0	12.5	0.5	26.0	3.1
SP-PVA-Source 30	Diffusion	26.8	0.352	24.8	0.8	0.5	5.0	0.5	10.2	1.5
Source 15S	Diffusion	15.9	0.302	6.1	4.5	0.5	20.5	1.5	–	–
Source 30S	Diffusion	28.0	0.300	14.4	1.5	0.0	8.0	1.0	17.0	2.9
SP-PVA-PLRP4000s 15–25 μm	Diffusion–convection	24.9	0.271	13.5	4.1	0.5	11.6	1.5	18.2	2.0
SP-PVA-PLRP4000s 50–70 μm	Diffusion–convection	72.5	0.263	2.7	0.6	0.0	1.8	0.5	3.5	1.0
POROS 20SP	Diffusion–convection type 1	21.8	0.317	9.5	2.5	0.0	12.0	0.75	26.0	2.6
SP POROS 20 OH	Diffusion–convection type 2	26.6	0.2521	8.4	2.0	1.0	6.5	1.5	13.0	1.75

[a] Calculated for linear region only.

3.3. Plate height analysis

Plate heights were measured for a small sized solute ($NaNO_3$) to establish the overall column efficiency and then for two proteins of substantially different sizes, lysozyme and IgG (lysozyme: M_r 14 300, D_{free} $11.2 \cdot 10^{-11}$ m^2/s; IgG: M_r 150 000, D_{free} $4.0 \cdot 10^{-11}$ m^2/s [16]). Fig. 2 compares the calculated plate height for the protein pulses with the measured plate height and Table 2 summarises the Van Deemter equation parameters. Application of lysozyme pulses produced elution chromatographic peaks with greater degrees of symmetry than those obtained with the use of IgG. The degree of peak symmetry decreased with the application of IgG on larger supports at higher flow-rates.

It can be seen from Fig. 2 that there is a linear relationship between superficial velocity and plate height for each bed of diffusion particles. The plate height at a given superficial velocity is highly dependent on particle size. The Source 15 matrices (diameter approximately 15 μm) had plate heights substantially lower than the larger Source 30 particles (diameter approximately 30 μm) and the Source 15S particle had plate heights comparable with the smaller diffusion–convection particles. Plate height increased more rapidly with an increase in mobile phase superficial velocity with larger particles.

The bead tortuosity factors, τ', which are directly related to the pore diffusivity, were similar for both lysozyme and IgG on the diffusion SP derivatised coated diffusion matrices, and were generally in the range of 1.0 to 2.4 with the exception of the POROS 20SP type 1 matrix. With similar tortuosity factors lysozyme pore diffusivity is higher than the IgG pore diffusivity in all matrices and this is due to the free diffusivity of lysozyme being nearly three-times larger than that of IgG. The tortuosity factors of the diffusion–convection supports varied slightly more than the diffusion supports but overall these tortuosity factors were similar to those measured by McCoy et al. [8] who calculated lysozyme tortuosity factors, using a monodisperse pore structure model, to be about 1.26 for the POROS 20 type 1 support and 2.15 for the POROS 20 type 2 support.

As expected, the split ratio values were zero for diffusion beads, but were larger for the diffusion–convection matrices. The two values of the split ratios measured with the two proteins were similar to each other, suggesting that they accurately describe the fraction of liquid that flows through the particles. However, the values obtained here are generally higher than those obtained by McCoy et al. [8] who obtained split ratios of about 0.0037 for the POROS 20SP type 1 matrices and split ratios of 0.0071 and 0.0019 for type 1 and type 2 POROS reversed-phase supports, respectively. These values were obtained using a plate height analysis based on a monodisperse pore structure with 1–10 μl injections of 1 mg/ml lysozyme, IgG and α-chymotrypsinogen A on a 100×4.6 mm column.

The plate height of diffusion–convection supports becomes independent of flow-rate at high flow-rates if described by a monodisperse Van Deemter pore model. With the incorporation of microparticle pore diffusion resistance in a bidisperse pore model, plate height will not be independent of flow-rate at high flow-rates. It can be seen from Fig. 2, however, that the experimental diffusion–convection support plate heights show a high degree of independence from flow-rate at high flow-rates indicating that the effect of microparticle pore diffusion on overall plate height is small over the range of flow-rates used in these experiments. The particles with a high split ratio, POROS 20SP type 1 and SP-PVA-PLRP4000s 15–25 μm supports, displayed plate height independent of flow-rate even at relatively low superficial velocities of 600 cm/h.

With the SP-PVA-PLRP4000s 15–25 μm and the POROS 20SP type 1 particles a plateau plate height of about 1.25 mm is seen indicating that a low plate height can be maintained at high flow-rates. The larger diffusion–convection particle PLRP4000s 50–70 μm had a low split ratio and consequently a higher plate height. This lower split ratio resulted in the convection effect not having significant influence until superficial velocities of 1000 cm/h had been reached and this is consistent with results shown by Weaver and Carta [15] who found no indication of convective mass transport in POROS 50 media (diffusion–convection particles of diameter 50 μm, type 1 matrix) until a superficial velocity of 5000 cm/h had been reached. It is noted that the plate

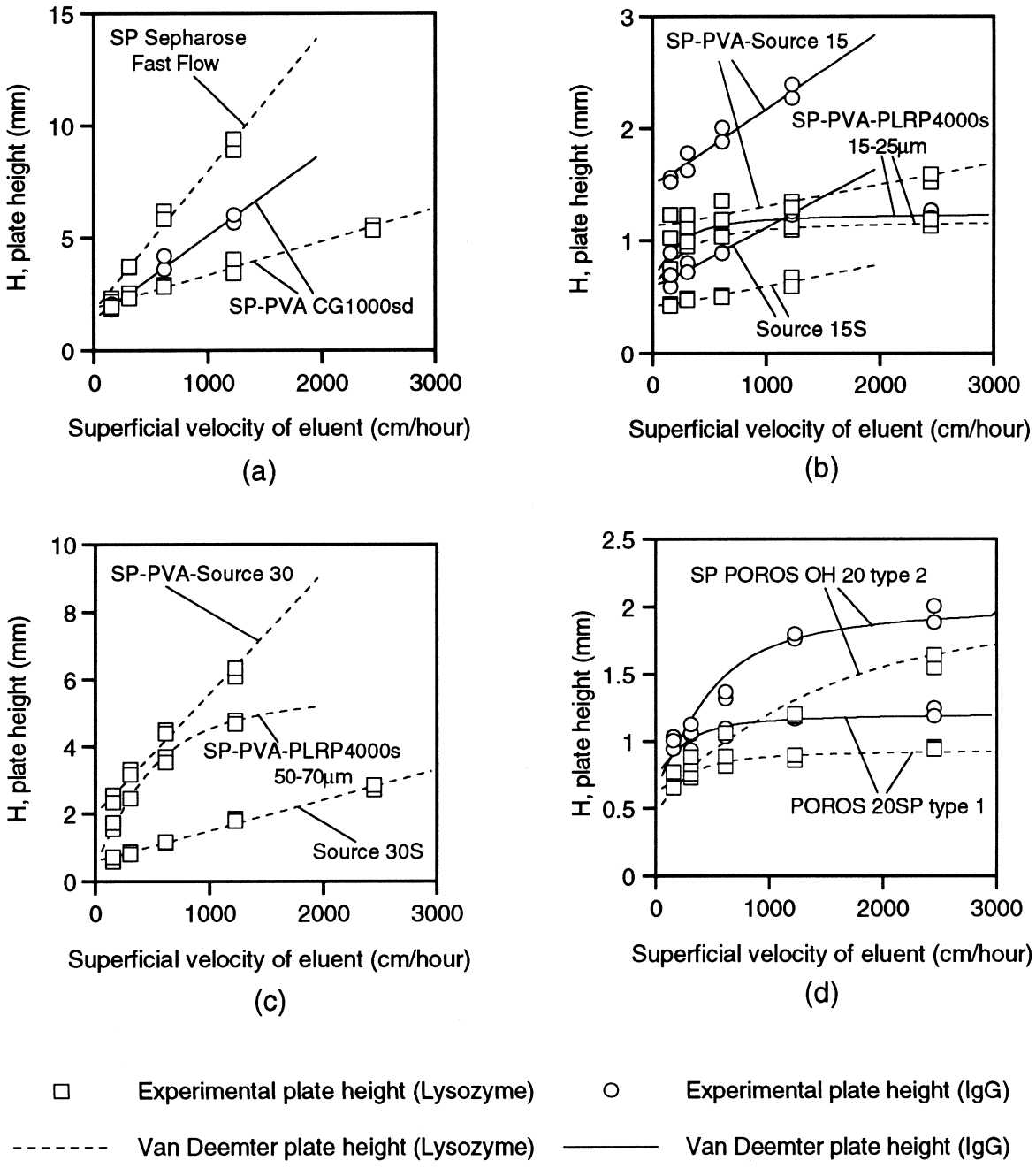

Fig. 2. Plate heights for lysozyme and IgG on SP and S derivatised chromatography supports under non-retaining conditions. Column plate heights with protein solutes were determined by applying a 25 μl pulse of protein [lysozyme or IgG (1 mg/ml) in 1.5 *M* NaCl in 20 m*M* phosphate buffer, pH 6.0] at varying flow-rates (0.5, 1, 2, 4 and 8 ml/min corresponding to superficial velocities of 153, 306, 1222 and 2445 cm/h) through an HR5/10 column (100×5 mm, 2 ml column volume). Plate height calculations and predictions were carried out as described in Section 2.3.4.

Table 2
Van Deemter equation parameters used to model plate heights of chromatography particles

Bead type	Column efficiency ($NaNO_3$) (mm)	Protein	Packing constant (A) (mm)	Effective pore diffusivity (D_p) ($\cdot 10^{-11}$ m^2/s)	Tortuosity factor (τ')	Split ratio (α)	Experimental plate height at $u = 1222$ cm/h (mm)
SP Sepharose Fast Flow[a]	0.30	Lysozyme	1.80	10.4	1.08	0.0	9.20
		IgG[c]	–	–	–	–	–
SP-PVA-CG1000sd[a]	0.09	Lysozyme	1.88	5.30	2.11	0.0	3.70
		IgG	1.42	2.13	1.88	0.0	5.80
SP-PVA-Source 15[a]	0.09	Lysozyme	1.11	7.17	1.56	0.0	1.32
		IgG	1.48	2.00	2.00	0.0	2.32
SP-PVA-Source 30[a]	0.20	Lysozyme	2.00	1.15	9.74	0.0	6.21
		IgG[c]	–	–	–	–	–
Source 15S[a]	0.08	Lysozyme	0.40	7.51	1.49	0.0	0.62
		IgG	0.57	2.68	1.49	0.0	1.23
Source 30S[a]	0.17	Lysozyme	0.64	6.03	1.86	0.0	1.83
		IgG[c]	–	–	–	–	–
SP-PVA-PLRP4000s 15–25 μm[b]	0.15	Lysozyme	0.58	4.62	2.42	0.0073	1.10
		IgG	0.65	3.75	1.07	0.0073	1.22
SP-PVA-PLRP4000s 50–70 μm[b]	0.43	Lysozyme	0.54	7.79	1.44	0.0024	4.74
		IgG[c]	–	–	–	–	–
POROS 20SP type 1[b]	0.16	Lysozyme	0.45	3.70	3.03	0.0078	0.87
		IgG	0.73	3.97	1.01	0.0078	1.17
SP POROS 20 OH type 2[b]	0.19	Lysozyme	0.60	10.9	1.03	0.0032	1.20
		IgG	0.64	4.00	1.00	0.0036	1.78

[a] Support was characterised using Van Deemter equation describing monodisperse pore structure.
[b] Support was characterised using Van Deemter equation describing bidisperse pore structure.
[c] Values could not be determined as peaks were asymmetrical.

heights of the diffusion–convection supports at a high superficial velocity are similar regardless of protein type. This is because protein diffusivity becomes unimportant at high flow-rates and the split ratios associated with each support type is independent of the nature of the solute.

3.4. Ionic capacities and isotherm parameters

The ionic capacities and Langmuir isotherm values for each of the SP and S derivatised beads are displayed in Table 3. The ionic capacities do not vary substantially between bead types, but the amount of protein that could be bound to the matrices varied considerably. It can be seen that the protein binding capacity for the PVA-coated matrices are lower than the commercially available matrices, even though the ionic capacities are much the same. The ratio of maximum protein binding capacity to bead ionic charge (which indicates how much protein binds to each ionic group and is therefore a measure of charge binding efficiency) is shown in Table 3. It can be seen that the values of protein/charge binding ratios for SP-PVA-PS–DVB matrices are about half of those obtained from commercial matrices. The binding efficiencies of the PVA coated matrices are low and this could be due to the chemical derivatisation with SP groups not being fully optimised, resulting in localised areas of very high ionic capacities, or with SP groups which have been immobilised into the PVA layer in locations where no subsequent interaction with proteins is possible.

The diffusion matrices had higher protein binding capacities for both lysozyme and IgG than the

Table 3
Ionic capacities, isotherm parameters and recoveries

Bead name	Ionic capacity (mmol/ml bed)	Protein	Maximum adsorption capacity (Q_m) (mg/ml)	Dissociation constant (K_d) (mg/ml)	Binding density (Q_m/ionic capacity) (mg/mmol)	Protein recovery (%)
SP Sepharose Fast Flow	0.229	Lysozyme	140.0	0.046	611.4	100.1
		IgG	115.0	0.555	502.2	100.4
SP-PVA-CG1000sd	0.176	Lysozyme	35.5	0.031	201.7	103.6
		IgG	45.0	0.078	255.7	104.4
SP-PVA-Source 15	0.182	Lysozyme	29.5	0.010	162.1	103.0
		IgG	36.7	0.040	201.6	101.0
SP-PVA-Source 30	0.263	Lysozyme	39.5	0.031	150.2	98.2
		IgG	49.0	0.059	186.3	100.8
Source 15S	0.299	Lysozyme	68.0	0.061	227.4	108.1
		IgG	62.0	0.215	207.4	102.3
Source 30S	0.240	Lysozyme	80.0	0.023	333.3	101.3
		IgG	72.0	0.205	300.0	94.1
SP-PVA-PLRP4000s 15–25 μm	0.202	Lysozyme	16.8	0.009	83.2	104.2
		IgG	20.0	0.100	99.0	103.5
SP-PVA-PLRP4000s 50–70 μm	0.140	Lysozyme	15.9	0.006	113.6	100.5
		IgG	17.0	0.064	121.4	104.6
POROS 20SP type 1	0.194	Lysozyme	40.0	0.007	206.2	105.3
		IgG	38.5	0.089	198.5	105.6
SP POROS 20 OH type 2	0.117	Lysozyme	21.0	0.008	179.5	102.4
		IgG	28.6	0.095	244.4	104.4

diffusion–convection matrices. Diffusion SP-PVA coated matrices had IgG saturation capacities in the region of up to 50 mg/ml, and lysozyme capacities up to 40 mg/ml whereas the SP-PVA coated diffusion–convection matrices had IgG capacities in the region of up to 20 mg/ml and 18 mg/ml for lysozyme. The same trend of adsorption capacities is seen with the commercially available matrices, in which the POROS 20SP type 1 matrix has capacities for both lysozyme and IgG of about 40 mg/ml compared to the capacities for lysozyme and IgG on Source S beads of up to 80 mg/ml. The capacity on SP Sepharose Fast Flow for lysozyme is around 140 mg/ml and it is 115 mg/ml for IgG. These values compare with the manufacturer's results which state that the protein capacity of POROS 20SP type 1 matrices to be 45 mg/ml (protein unknown) [17], Source 15S and Source 30S matrices to be greater than 25 mg/ml and 80 mg/ml (lysozyme, conditions unknown) [16] and SP Sepharose Fast Flow to be 120 mg/ml (bovine serum albumin, conditions unknown) [16]. The protein/charge binding ratio is greater in the diffusion beads than in the diffusion–convection beads and this is probably due to the ionic groups in the diffusion beads being spread over a much larger surface area.

3.5. Protein recoveries

Table 3 shows the recoveries of lysozyme and IgG from the SP and S derivatised matrices. The recovery for all matrices were approximately 100% indicating that there is no irreversible non-specific adsorption of these proteins to any of these adsorbents. This is further evidence that PVA coating of PS–DVB matrices is an effective method for shielding their hydrophobic surfaces.

3.6. Frontal analysis

The plate heights of diffusion–convection matrices become independent of flow-rate at high flow-rates and this ensures that the diffusion–convection matrices have lower plate heights than diffusion matrices at higher flow-rates. However, the diffusion matrices have a greater number of binding sites, and have a greater protein binding capacity than corresponding diffusion–convection matrices. The rate at which protein adsorbs on these matrices is a function of plate height and, as the plate height increases, it is expected that the dynamic capacities should drop. It would also be expected that the dynamic capacities of diffusion matrices will drop more quickly than with comparable diffusion–convection matrices. Figs. 3 and 4 and Table 4 show the frontal analysis results on SP and S derivatised chromatography matrices. Samples of typical frontal curves obtained are shown in Fig. 3.

It can be seen from Fig. 4 and Table 4 that the decline in 5% dynamic capacity with increase in flow-rate is dependent on both protein type and bead type. Lysozyme is a small protein (M_r 14 300) with a corresponding high diffusion coefficient and is able to penetrate particles easily, even if the particles have long pore lengths and small pore diameters. It is seen that the drop in lysozyme dynamic capacity with increase in flow-rate is small for most bead types whether they are diffusion or diffusion–convection matrices. This has been observed in previous work [18]. The only real exceptions to this observation are the SP-PVA-Source 30 matrices and the SP Sepharose Fast Flow matrices. The agarose-based SP Sepharose Fast Flow matrix shows a large drop in dynamic capacity with an increase in flow-rate. At 306 cm/h flow-rate the IgG adsorption has dropped to about 14% that of the equilibrium capacity and at 1222 cm/h the lysozyme capacity has dropped to about 17% that of equilibrium and IgG adsorption to about 5%. This may be due to the combination of the small pores of the matrix (400 Å) [19], the large particle size (100 μm) and the compressibility of agarose at high flow-rates. The amounts of protein adsorbed onto the SP-PVA-Source 30 matrices are much lower than those onto the comparable CG1000sd or Source 15 matrices and this is probably a result of the porous nature of the bead. The pore size of the Source 30 matrices appears much smaller than those of other polystyrenic matrices (Fig. 1). However it is important to note that at even the highest flow-rates, the dynamic capacities of lysozyme on the diffusion matrices are higher than on comparable diffusion–convection matrices.

IgG, however, is a much larger molecule than lysozyme (IgG M_r 150 000) and has a smaller diffusion coefficient (about a third that of lysozyme). Consequently, the binding capacity of IgG on SP and S derivatised matrices drops more quickly than that for lysozyme adsorption. For the diffusion particles, the dynamic capacity is about 60–80% of equilibrium capacity at a flow-rate of 306 cm/h (not including the Source 30 matrices or the SP Sepharose Fast Flow) compared to lysozyme adsorption of 70–90% at the same flow-rate. At the fastest flow-rate, 2445 cm/h, the dynamic capacity dropped to about 17–40% of equilibrium capacity for the same diffusion beads, compared to lysozyme adsorption of 55–70% at the same flow-rate. Mass transfer of IgG into diffusion–convection matrices is mainly by convective means at the higher superficial velocities (when diffusion mass transfer becomes negligible). It can be seen that the dynamic capacity does not drop significantly with an increase in applied flow-rate. The only exception being the 50–70 μm sized PLRP4000s matrix which has mass transfer restrictions into it because of the large particle diameter. The 5% dynamic capacities for IgG with the smaller diffusion–convection particles are slightly lower than with the smaller diffusion particles (Source 15), even at the highest flow-rate. However the 5% dynamic capacities for IgG with the smaller diffusion–convection matrices are higher than those obtained with the larger diffusion particles (CG1000sd and Source 30 particles).

3.7. Resolution of protein peaks

Lysozyme and cytochrome *c* were chosen to measure the resolution between proteins as they are similar sized proteins, thus reducing size exclusion effects. This is desirable as it ensures the same available binding surface area for both proteins. Samples of typical chromatograms obtained are shown in Fig. 5. Fig. 6a and Fig. 6b show a summary of the values of the resolutions achieved.

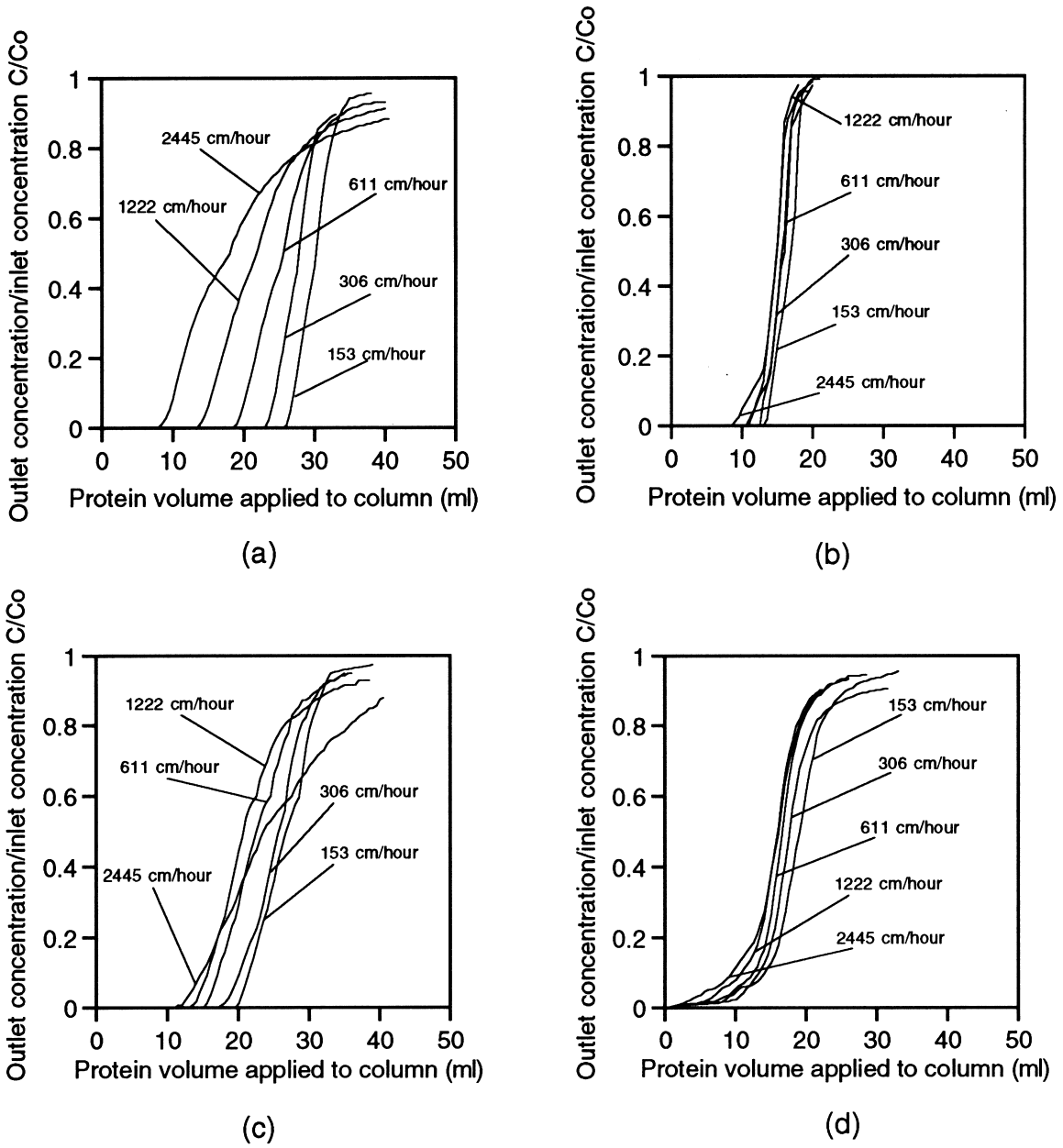

Fig. 3. Breakthrough curves of lysozyme and IgG on SP and S derivatised chromatography supports. The figures correspond to: (a) lysozyme (1 mg/ml) applied to SP-PVA-Source 30, (b) lysozyme (1 mg/ml) applied to SP-PVA-PLRP4000s 15–25 μm matrices, (c) IgG (2 mg/ml) applied to Source 15S matrices and (d) IgG (2 mg/ml) applied to POROS 20SP type 1 matrices. Lysozyme (1 mg/ml, 2 mg/ml) or IgG (1 mg/ml, 2 mg/ml) in 20 m*M* phosphate buffer pH 6.0 was applied to SP or S derivatised matrices in an HR5/5 column (50×5 mm, 1 ml column volume) at flow-rates in a strict order of 1, 1, 0.5, 2, 4, 8 and 1 ml/min corresponding to a superficial velocities of 306, 306, 153, 611, 1222, 2445 and 306 cm/h.

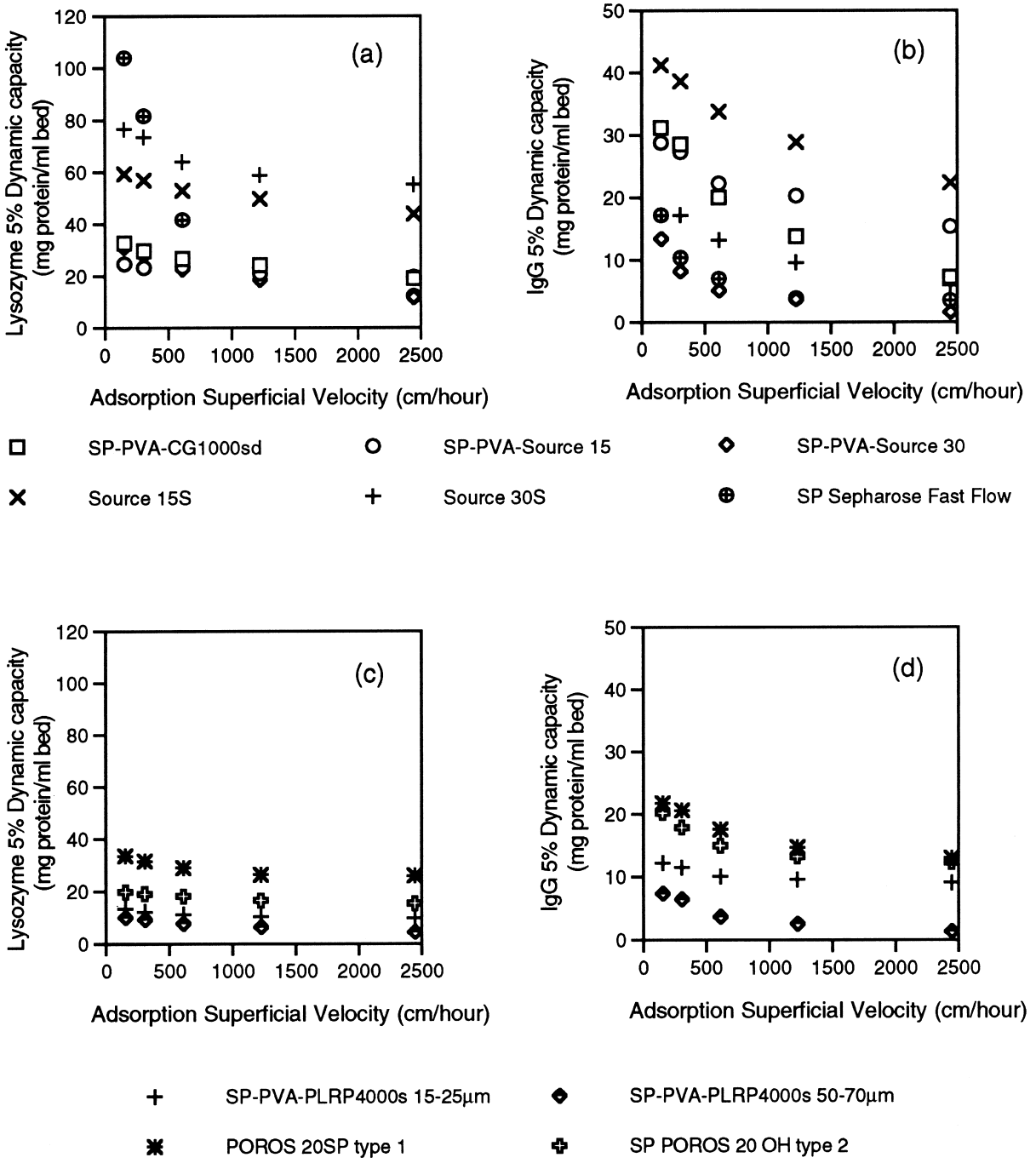

Fig. 4. 5% Dynamic capacities of lysozyme and IgG on SP or S derivatised chromatography supports. Figures correspond to: (a) lysozyme on diffusion matrices, (b) IgG on diffusion matrices, (c) lysozyme on diffusion–convection matrices and (d) IgG on diffusion–convection matrices. Lysozyme (1 mg/ml, 2 mg/ml) or IgG (1 mg/ml, 2 mg/ml) in 20 m*M* phosphate buffer pH 6.0 was applied to SP or S derivatised matrices in an HR5/5 column (50×5 mm, 1 ml column volume) at flow-rates in a strict order of 1, 1, 0.5, 2, 4, 8 and 1 ml/min corresponding to a superficial velocities of 306, 306, 153, 611, 1222, 2445 and 306 cm/h. Dynamic capacities were calculated as described in Section 2.3.4.1.

Table 4
Dynamic capacities of SP derivatised modified matrices

Bead name	Protein	Equilibrium capacity at 1 mg/ml (mg/ml)	5% Dynamic capacity at 306 cm/h (mg/ml)	Dyn/ Equil. (%)	%% Dynamic capacity at 1222 cm/h (mg/ml)	Dyn/ Equil. (%)	5% Dynamic capacity at 2445 cm/h (mg/ml)	Dyn/ Equil. (%)
SP Sepharose Fast Flow	Lysozyme	134.0[a]	81.7	61.0	23.3	17.4	12.3	9.2
	IgG	74.0[a]	10.4	14.1	3.9	5.3	3.5	4.7
SP-PVA-CG1000sd	Lysozyme	34.4	29.8	86.6	24.3	70.6	19.2	55.8
	IgG	41.7	28.5	68.3	13.8	33.1	7.3	17.5
SP-PVA-Source 15	Lysozyme	29.2	23.4	80.1	21.1	72.2	19.7	67.5
	IgG	35.3	27.3	77.3	20.3	57.5	15.4	43.6
SP-PVA-Source 30	Lysozyme	38.3	28.2	73.6	18.6	48.6	11.8	30.8
	IgG	46.3	8.2	17.7	3.7	8.0	1.6	3.5
Source 15S	Lysozyme	66.0[a]	57.0	86.4	49.8	75.5	43.9	66.5
	IgG	56.0[a]	38.6	68.9	28.9	51.6	22.4	40.0
Source 30S	Lysozyme	79.1[a]	73.5	92.9	58.9	74.5	55.2	69.8
	IgG	65.3[a]	17.2	26.3	9.6	14.7	5.9	9.0
SP-PVA-PLRP4000s 15–25 μm	Lysozyme	16.7	12.2	73.1	10.3	61.7	9.8	58.7
	IgG	18.2	11.5	63.2	9.6	52.7	9.1	50.0
SP-PVA-PLRP4000s 50–70 μm	Lysozyme	15.5	9.2	59.4	6.4	41.3	4.4	28.4
	IgG	16.5	6.5	39.4	2.6	15.8	1.4	8.5
POROS 20SP type 1	Lysozyme	39.7	31.4	79.1	26.3	66.2	25.8	65.0
	IgG	35.4	20.7	58.5	14.7	41.5	13.0	36.7
SP POROS 20 OH type 2	Lysozyme	20.8	19.0	91.3	16.5	79.3	15.3	73.6
	IgG	26.1	17.9	68.6	13.2	50.6	12.3	47.1

[a] Determined at equilibrium concentration of 2 mg/ml as frontal analysis was conducted with protein concentration of 2 mg/ml.

SP Sepharose Fast Flow showed no peak resolution at all protein loadings and all flow-rates tested (results not shown). However it is likely that the lack of resolution is due to thermodynamic effects rather than kinetic effects, as under different adsorption/elution conditions resolutions of these proteins on SP Sepharose Fast Flow can be achieved [20]. It can be seen in Fig. 6a that for the larger diffusion particles (Source 30 and CG1000sd), the resolution of analytical quantities of protein drops substantially with an increase in flow-rate. The smaller diffusion matrices (Source 15) show a smaller reduction in resolution with an increase in flow-rate. The resolution drops with an increase in the amount of applied protein, but the drop in resolution with a subsequent increase in superficial velocity is smaller than at analytical loadings. At all levels of protein loading, resolution between the two proteins was achieved with all the diffusion matrices at all superficial velocities. Generally, the resolutions for the PVA-coated matrices derivatised with SP (using the cyanogen chloride method as described earlier) (SP-PVA-PS–DVB) showed higher resolutions than commercial SP or S matrices.

The resolutions obtained on diffusion–convection matrices are shown in Fig. 6b and it can be seen that for analytical protein loadings, the drop in resolution with an increase in flow-rate is generally small for all the diffusion–convection matrices except the POROS type 2 matrix. The POROS 20 type 2 matrix throughpores have smaller diameters than those on the type 1 matrices and with these smaller throughpores, intra-particle mass transfer is less rapid. Consequently plate height increases more quickly with an increase in superficial velocity than with the POROS 20 type 1 matrices. Most of the diffusion–convection matrices were unable to achieve peak resolution at preparative protein loadings. Only two

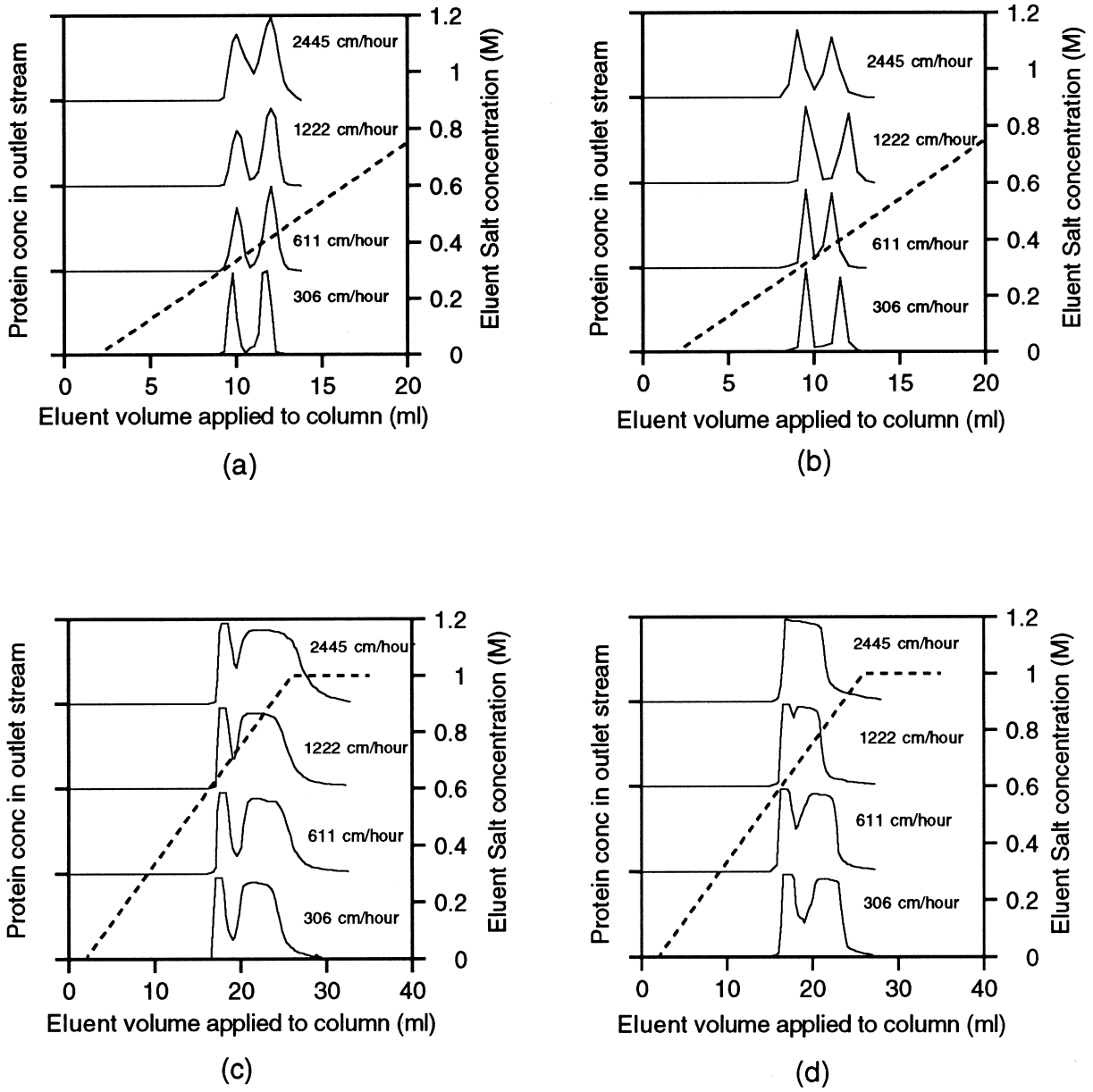

Fig. 5. Resolutions of lysozyme and cytochrome *c* on SP and S derivatised chromatography supports. The chromatograms correspond to: (a) 0.05 mg total protein on Source 30S matrices, (b) 0.05 mg total protein on POROS 20SP type 1 matrices, (c) 20 mg total protein on SP-PVA-CG1000sd matrices and (d) 20 mg total protein on SP POROS 20 OH type 2 matrices. Each SP and S derivatised matrix was loaded into an HR5/10 column (100×5 mm, 2 ml bed volume) and a volume of cytochrome *c* and lysozyme solution in 20 m*M* phosphate buffer pH 6.0 was applied to the column (total protein mass loading 0.05 mg, 0.5 mg, 2. 5mg, 5.0 mg, 10.0 mg and 20.0 mg, lysozyme and cytochrome *c* at equal concentrations). The protein was applied at a flow-rate of 1 ml/min, 306 cm/h. After the protein was applied, the column was washed with 4 ml of buffer (1 ml/min, 306 cm/h) and then a buffer gradient was applied to the column at a variety of flow-rates, with a gradient change of 0–1 *M* NaCl in 20 m*M* phosphate buffer pH 6.0 in 12 column volumes (24 ml).

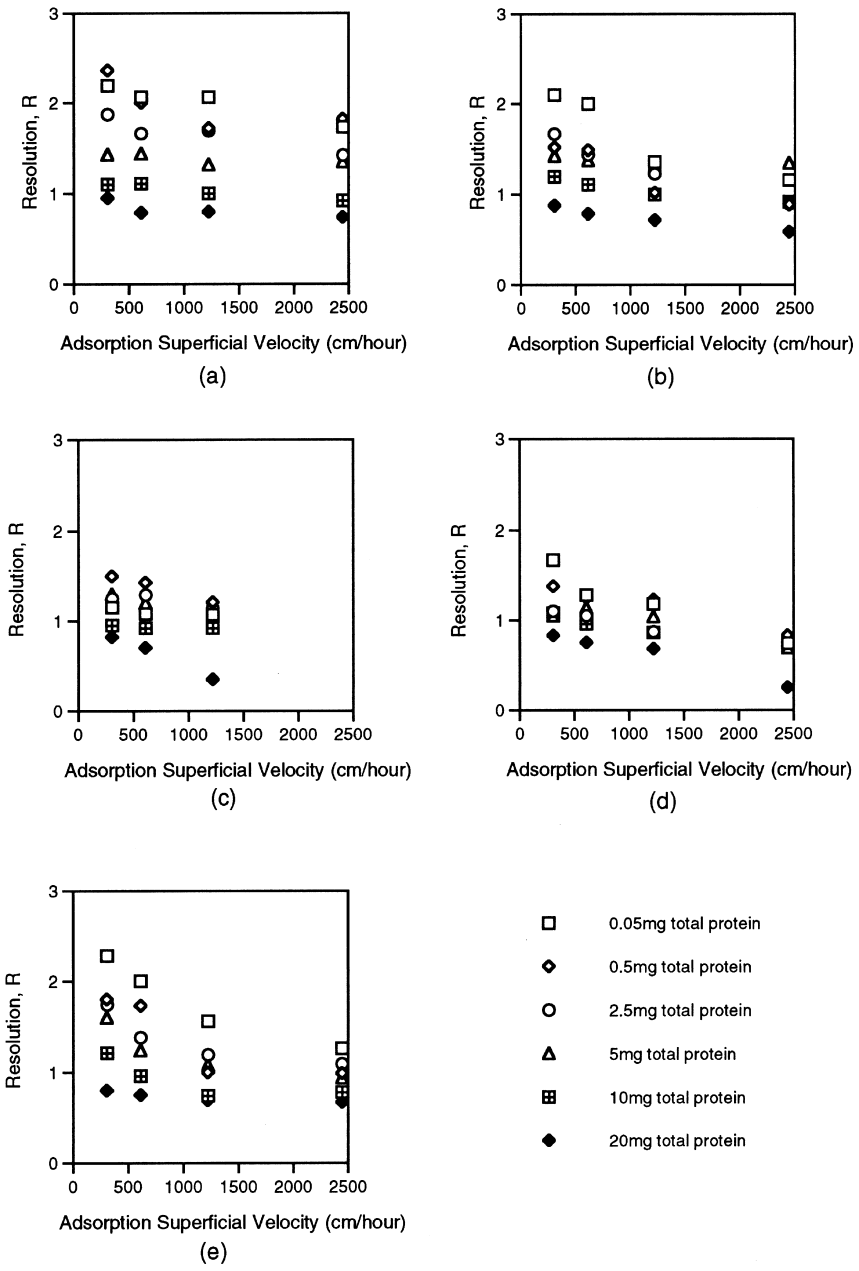

Fig. 6. Summary of peak resolution for SP or S derivatised chromatography supports. The figures correspond to: (a) resolutions on SP-PVA-Source 15 matrices, (b) resolutions on SP-PVA-Source 30 matrices, (c) resolutions on Source 15S matrices, (d) resolutions on Source 30S matrices and (e) resolutions on SP-PVA-CG1000sd matrices, (f) resolutions on SP-PVA-PLRP4000s 15–25 μm matrices, (g) resolutions on SP-PVA-PLRP4000s 50–70 μm matrices, (h) resolutions on POROS 20SP type 1 matrices and (i) resolutions on SP POROS 20 OH type 2 matrices. Each SP and S derivatised matrix was loaded into an HR5/10 column (100×5 mm, 2 ml bed volume) and a volume of cytochrome *c* and lysozyme solution in 20 m*M* phosphate buffer pH 6.0 was applied to the column (total protein mass loading 0.05 mg, 0.5 mg, 2.5 mg, 5.0 mg, 10.0 mg and 20.0 mg, lysozyme and cytochrome *c* at equal concentrations). The protein was applied at a flow-rate of 1 ml/min, 306 cm/h. After the protein was applied, the column was washed with 4 ml of buffer (1 ml/min, 306 cm/h) and then a buffer gradient was applied to the column at a variety of flow-rates, with a gradient change of 0–1 *M* NaCl (0–1.5 *M* NaCl for resolution studies on SP-PVA-Source 15 and 30 matrices) in 20 m*M* phosphate buffer pH 6.0 in 12 column volumes (24 ml).

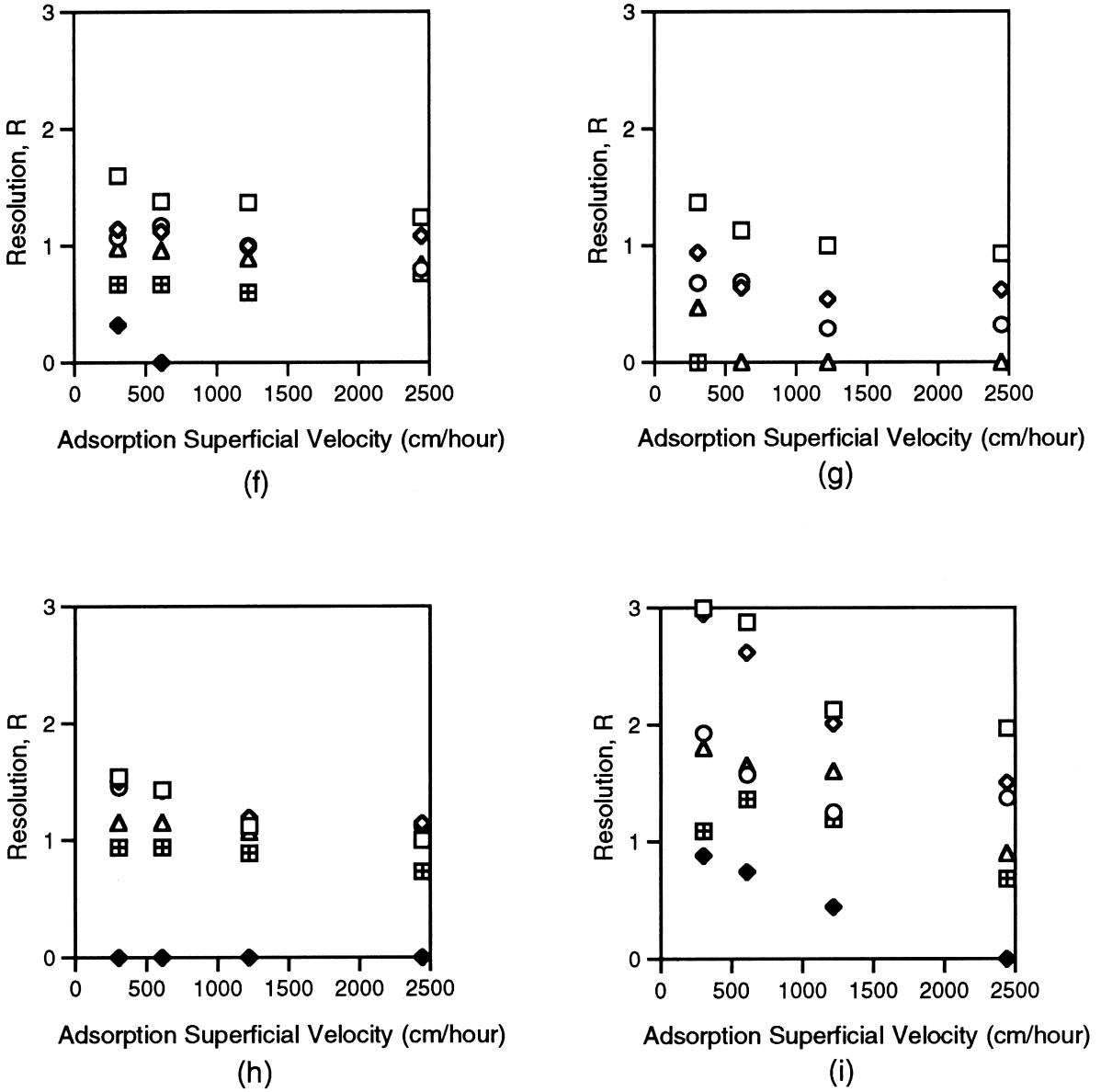

Fig. 6. (*continued*)

bead types, PLRP4000s 15–25 μm and SP POROS 20 OH type 2 could resolve 20 mg of applied protein, and the PLRP4000s 15–25 μm matrix showed no signs of resolution for this protein loading at flow-rates greater than 611 cm/h. The POROS 20 type 2 matrix showed no resolution of this loading at a superficial velocity of 2445 cm/h.

Fig. 6a and Fig. 6b indicate that diffusion–convection particles are not as good as diffusion particles at achieving peak resolution at preparative levels of applied protein. This is a result of the higher dynamic binding capacity of the diffusion particles. For analytical quantities of applied protein (0.05 mg) the differences between the two matrix types is small, with the diffusion–convection matrices providing better resolution at higher superficial velocities than the larger diffusion matrices, but about the same resolution as the smaller Source 15 matrix. However the diffusion–convection matrices can be operated at a higher superficial velocity than the smaller Source 15 matrices without incurring excessive pressure drop.

4. Conclusions

A comprehensive study has been undertaken on various diffusion and diffusion–convection particles to investigate the plate height parameters, capacities, dynamic capacities and resolutions on each matrix type. It has been shown that plate heights obtained follow a model derived by Carta and Rodrigues [28] for both diffusion and diffusion–convection particles. A bidisperse model was used to estimate the characteristics of the diffusion–convection supports.

The choice of particle size is important in determining the most desirable matrix for a particular application. Source 15 particles have low plate heights and high binding capacities and therefore have high dynamic capacities. However the back pressure associated with these beads is high. Larger diffusion matrices have higher plate heights and a dynamic capacity that is more dependent on flow-rate. Diffusion–convection matrices have low equilibrium binding capacities but allow convective flow through the particles at high flow-rates thus improving the rate of mass transfer. Larger 50–70 μm diffusion–convection matrices are inferior to smaller diffusion–convection media as the plate height associated with these beads is high due to their larger size. In addition, the low split ratio of these larger particles means that the convective flow regime is not easily reached. Equilibrium capacities of the larger diffusion–convection matrices are also low.

Although diffusion–convection matrices show more rapid mass transfer to the internal binding sites than diffusion matrices, especially at high flow-rates, their low overall binding capacity means that in most operating regimes their dynamic capacity is lower than for comparable diffusion matrices. The resolution study using lysozyme and cytochrome *c* showed that for preparative separations, the larger surface area available on the diffusion matrices provides better resolution than diffusion–convection matrices. At analytical level, however, the diffusion–convection matrices will be able to achieve high resolution for all protein sizes at fast flow-rates.

5. List of symbols

A	Packing constant (mm)
$a_{0.1}$	Distance between peak front and peak maximum at 0.1 peak height
B	Axial diffusion term in Eq. (6)
b	Term defined by Eq. (13)
$b_{0.1}$	Distance between peak maximum and peak tail at 0.1 peak height
c'	Solute concentration in particle throughpores (mg/ml)
C	Concentration of protein in solution (mg/ml)
C_{ads}	Adsorption kinetic term in Eq. (6)
C_f	External stationary phase film term in Eq. (6)
C_p	Pore diffusion term in Eq. (6)
C_s	Concentration of bound protein (mg/ml)
D_c	Solute diffusivity in microparticle (m^2/s)
D_{free}	Free solute diffusivity (m^2/s)
D_p	Solute diffusivity in particle pore (m^2/s)
$f(\lambda)$	Convective enhancement factor
H	Plate height (mm)
K	Bed permeability (cm^2/h bar)
K	Henry's constant ($K=0$ for unretained solute)

K'	Distribution coefficient between throughpore and microparticle
K_d	Dissociation constant (mg/ml)
L_0	Column length (mm)
N	Plate number
q	Total solute microparticle concentration (mg/ml microparticle)
Q_m	Maximum binding capacity (mg/ml)
R	Protein resolution
R_m	Microparticle radius (m)
R_p	Particle radius (m)
S	Symmetry coefficient
T	Diffusional time constant
t_r	Peak mean residence time
u	Mobile phase superficial velocity (cm/h)
v_p	Intraparticle velocity (m/s)
w	Width of solute peak at baseline
$w_{0.5}$	Width of peak at half peak height
α	Split ratio, volume fraction intraparticle flow
ΔP	Column pressure drop (bar)
ε	Bed voidage
ε'	Throughpore voidage in particle
ε''	Pore voidage in microparticle
ε_p	Total particle voidage (porosity)
λ	Intraparticle Peclet number
σ^2	Peak width variance
τ	Pore tortuosity
τ'	Tortuosity factor

Acknowledgements

The authors wish to acknowledge financial support for this work from the BBSRC (UK) and are grateful to Polymer Laboratories and Pharmacia Biotech for the gifts of adsorbents.

References

[1] J.C. Moore, J. Polymer Sci., Part A 2 (1964) 835.
[2] S.K. Paliwal, M. De Frutos, F.E. Regnier, Methods Enzymol. 70 (1996) 133.
[3] R. Janzen, K.K. Unger, H. Giesche, J.N. Kinkel, M.T.W. Hearn, J. Chromatogr. 397 (1987) 91.
[4] N.B. Afeyan, N.F. Gordon, I. Mazsaroff, L. Varady, S.P. Fulton, Y.B. Yang, F.E. Regnier, J. Chromatogr. 519 (1990) 1.
[5] L. Lloyd, F.P. Warner, J. Chromatogr. 512 (1990) 365.
[6] L. Lloyd, J. Chromatogr. 544 (1991) 201.
[7] E. McCarthy, G. Vella, R. Mhatre, Y.P. Lim, J. Chromatogr. A 743 (1996) 163.
[8] M. McCoy, K. Kalghatgi, F.E. Regnier, N.B. Afeyan, J. Chromatogr. A 743 (1996) 221.
[9] D.C. Nash, G.E. McCreath, H.A. Chase, J. Chromatogr. A 758 (1997) 53.
[10] D.C. Nash, H.A. Chase, J. Chromatogr. A 776 (1997) 55.
[11] G.E. McCreath, R.O. Owen, D.C. Nash, H.A. Chase, J. Chromatogr. A 773 (1997) 73.
[12] A.E. Rodrigues, ACS Symp. Ser. 635 (1996) 157.
[13] F. Helfferich, Ion Exchange, McGraw-Hill, New York, 1962.
[14] H.A Sober (Editor), CRC Handbook of Biochemistry: Selected Data for Molecular Biology, CRC Press, Cleveland, OH, 2nd ed., 1973.
[15] L.E. Weaver, G. Carta, Biotechnol. Prog. 12 (1996) 342.
[16] Pharmacia Information Booklet, Pharmacia Biotech, Uppsala, Sweden.
[17] PerSeptive Biosystems Information Booklet, PerSeptive Biosystems, Cambridge, MA, USA.
[18] D.C. Nash, H.A. Chase, J. Chromatogr. A 776 (1997) 65.
[19] TosoHaas Information Booklet, TosoHaas, Philadelphia, PA, USA.
[20] P.R. Levison, C. Mumford, M. Streater, A. Brandt-Nielsen, N.D. Pathirana, S.E. Badger, J. Chromatogr. A 760 (1997) 151.
[21] L. Varady, N. Mu, Y.B. Yang, S.E. Cook, N.B. Afeyan, F.E. Regnier, J. Chromatogr. 631 (1993) 107.
[22] H.A. Chase, in D. Naden and M. Streat (Editors), Ion Exchange Technology, Ellis Horwood, Chichester, 1984, pp. 400–406.
[23] H.A. Chase, J. Chromatogr. 297 (1984) 179.
[24] B.A. Bidlingmeyer, F.V. Warren, Anal. Chem. 56 (1984) 1583A.
[25] A.I. Liapis, M.A. McCoy, J. Chromatogr. A 660 (1994) 85.
[26] A.I. Liapis, M.A. McCoy, J. Chromatogr. 599 (1992) 87.
[27] P. Schneider, J.M. Smith, AIChE J. 14 (1968) 762.
[28] G. Carta, A.E. Rodrigues, Chem. Eng. Sci. 48 (1993) 3927.
[29] A.E. Rodrigues, B.J. Ahn, A. Zoulalian, AIChE J. 28 (1982) 541.
[30] R.F. Benenati, C.B. Brosilow, AIChE J. 8 (1962) 359.
[31] G.G. Brown, in Unit Operations, Wiley, New York, 1950.
[32] G.A. Heeter, A.I. Liapis, J. Chromatogr. 761A (1997) 35.